Scientific Visualization, 2023, volume 15, number 1, pages 1 - 16, DOI: 10.26583/sv.15.1.01

Visualization of Liquids Flows in Microfluidics and Plasma Channels in Nanosecond Spark Microdischarges by Means of Digital Microscopy

V.A. Dekhtyar[1,A], A.E. Dubinov[2,A, B]

[A] Russian Federal Nuclear Center – All-Russia Research Institute of Experimental Physics, 37 Mira Avenue, Sarov, Nizhny Novgorod Region 607188, Russia
[B] Sarov Institute of Physics and Technology – Branch of National Research Nuclear University "Moscow Engineering Physics Institute", 6 Dukhova Street, Sarov, Nizhny Novgorod Region 607186, Russia

[1] ORCID: 0000-0001-8890-612X, valerik128@mail.ru
[2] ORCID: 0000-0002-3185-7926, dubinov-ae@yandex.ru

Abstract

An application of digital optical microscopes for visualization of single-pulse or pulsed-periodic processes in microfluidics and physics of spark microdischarges is studied. Multiple examples of coagulation processes of liquid microvolumes, nanosecond spark discharges near liquid drops and plant living tissues in a cell-size level are provided.

Keywords: visualization, microfluidics, spark discharge, digital microscope.

1. Introduction

A main method of measurements is visualization of physical objects and processes. The method allows obtaining space-time, space-photometric, and other characteristics.

Microfluidics has lately got its development. A field is a comparatively new as hydrodynamics dealing with liquid drops, films, jets of liquid of less than 1 ml in volume [1,2]. The most important factors in microfluidics are viscosity, wettability, miscibility of different liquids, capillary phenomena, and volatility. Flows are often laminar in microfluidics since viscosity suppresses small-scale turbulent disturbances, and large-scale disturbances are impossible due to a small volume of liquid. Some of the known applications of technologies and devices of microfluidics are a jet printing, medicine synthesis in liquid and mixed forms, medical diagnosis based on bioliquids analysis, protection from virulferous microdrops (including drops with viruses of COVID-19), development of hydrophobic coverings, cleaning of surfaces, chemo-, bio- and agromicrotechnologies. Visualization of liquid flows in microfluidics allows understanding the description of physical processes.

A new field in physics and electrical discharge technology has recently appeared and is actively developing. It studies electrical microdischarges in interelectrode gaps of a submillimeter dimension [3–5]. Some of the types of microdischarges are a spark, a dielectric barrier discharge, a discharge with a microhollow cathode. The microdischarge have found its application in such fields as analytical chemistry, medicine, point light sources, etc. Visualization of microdischarges allows getting data about dimensions and forms of plasma channels, brightness, spectrum and other parameters.

New methods of regulation of hydrodynamic and physical-chemical processes in drops and liquid films have been lately proposed by means of nanosecond spark microdischarges [6–11]. A new plasma capillary effect was discovered during these studies; a peristaltic motion of drops sitting on a substrate under the action of microsparks was studied; the effect of the hysteresis inversion of contact angles at the drops motion up-

wards along an inclined plane was discovered. As a result of these studies, a new research direction appeared at the joint of the stated fields – microfluidics directed by microdischarges [12].

Besides, research have been introduced studying how a plasma of microdischarges affects living tissues of plants and animals on a cell-size level [13–16].

Such research is impossible without dynamical visualization of processes that is microvisualization. A digital colored high quality video-recording of processes with a good space and time resolution is necessary here [17,18]. Modern digital micrscopes with video cameras delivering images to computers during experiments allow getting necessary data. These data with results, e.g. of electrical measurements provide a detailed picture of the studied processes.

Some examples of video studies of processes in microfluidics and in the field of microdischarges performed by the authors by means of digital microscopes are provided in this work.

2. The used technical equipment of visualization

Cheap optical digital microscopes were used in the work. They can be bought in trading companies. Microscope brands and their main parameters are provided in the Tab. 1, their photos are in Fig.1. The microscopes were preliminary calibrated by means of test-objects.

The stated microscopes can operate in the mode I of a single photo image and in the mode II of a video recording as well. The mode I in cheap microscopes is not synchronized externally. Thus, the recording of photo images of single pulses, i.e. spark nanosecond discharges (the exact moment of their initiation is not defined) is not possible in the mode I. These images can be obtained only in the mode II.

We should note that nanosecond discharges create strong electromagnetic pickups near the microscope, and on the USB-cable connecting a microscope and a computer. It resulted in the computer operation and image recording failure. One of the images of a nanosecond spark discharge obtained on the 'Levenhuk' microscope is shown in Fig. 2a. There is a defect on this image in the form of a horizontal image cutoff as a result of a magnetic pickup. Therefore, special measures were taken to avoid failures: ground connection, screening and maximum moving away of the USB-cable from a discharge circuit. As a result, images were obtained without defects (Fig. 2b). An image similar to Fig. 2b, presented in [19], according to which it was possible to determine the diameter of the plasma channel of the spark ~20 μm.

Tab. 1. The used microscopes.

Microscope brand	Handheld digital microscope 'Celestron' (MODEL #44302-A)	Tabletop digital microscope 'Levenhuk' (MODEL D50L NG)
Camera	2MP CMOS Sensor – 1600x1200 pixel array (snapshots up to 5MB with interpolation)	2MP CMOS Sensor – 1600x1200 pixel array (snapshots up to 5MB with interpolation)
Recording velocity	20 fps	15 fps
Enlargement	regular 10 to 40x, maximal 150x	regular 40 to 640x, maximal 1285x (with the Barlow lens)
Weight and dimensions	0.420 kg, 21×15×5 cm	3.5 kg, 26×15.5×40 cm (package size)

a) b)

Fig. 1. The external view of the microscopes used in the operation: a) – 'Celestron' (MODEL #44302-A); b) – 'Levenhuk' (MODEL D50L NG).

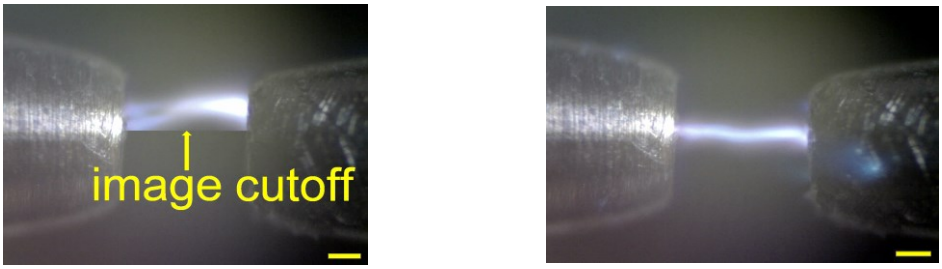

a) b)

Fig. 2. Samples of images of a nanosecond spark discharge between needle electrodes in the air of atmospheric pressure (obtained by the microscope 'Levenhuk', scale bar – 100 μm): a) – an image with a defect as an image cutoff; b) – an image without defects.

3. Visualization of the coagulation process of a sessile drop with a water film on a horizontal substrate

One of the main tasks of the applied microfluidics is coalescence and mixture of small portions of liquids [20,21]. It was discovered in the experimental studies of coalescence of two drops with different liquids that interpenetration of high-directivity single liquid jets happens before the mixture of liquids, one jet from each drop [22,23]. The experiments of coalescence of two drops sitting near on the substrate under the action of spark discharges were carried out in [24,25]. Coagulation of two sitting drops with convex curved boundaries was observed in all the above stated works and other known studies. The number of jets is one from each drop. In this work we tried to visualize coagulation of a sessile drop with a liquid film that had a straight-line boundary.

We prepared a water film on the steel surface of a flat vessel with the edges in the ellipse form of 6.4·7.4 cm, one of the film boundaries was straight-line. The film thickness was about 2 mm. Colored water was running from a hole of 1 mm diameter in the vessel bottom and was forming a drop of an increasing diameter. The similar scheme, when the liquid is running from a hole in the vessel bottom to perform a coagulation, was used in [26–28].

Crystals of $KMnO_4$ were used as a coloring agent. This coloring agent is convenient for visualization of water flow since only several crystals are needed to highlight the process. $KMnO_4$ molecules with a small concentration do not affect viscosity, density and water surface tension. Note that ions of MnO_4^- make water violet [29]. Therefore, water coloring by crystals for flow visualization is very popular among researchers [12,25,30–33].

In Fig.3 there are some characteristic snap-shots of video recording of one of the drop coagulation processes with water flow velocity from the hole of ~2 ml/min. The image in Fig. 3a is chosen for convenience as a start of time reading. A drop contact with a film and topological modification of a boundary happen very fast – for less than 50 ms (Fig. 3b,c). Then side jets appear (Fig. 3d) and are swirled in helical vortices, then some more jets appear between side ones (Fig. 3e,f). Multiple appearances of jets at the coagulation were observed here for the first time; it was well reproduced in many repetitions of this experiment at different distances between a straight line boundary and a hole, with different velocities of the water running from a hole.

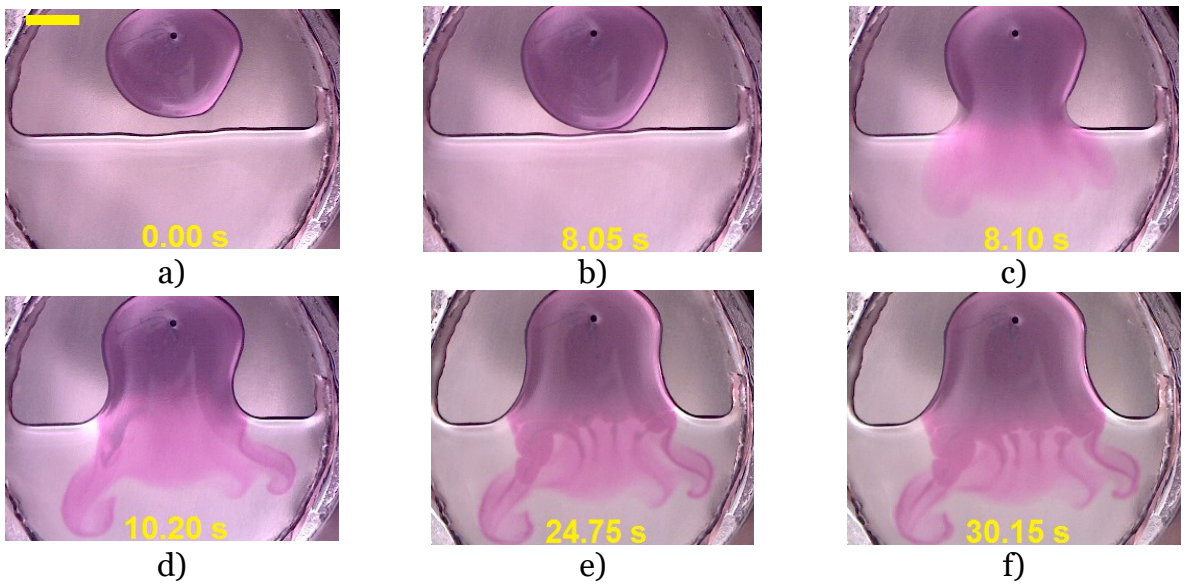

a) b) c)

d) e) f)

Fig. 3. Snapshots of video-recording of one of the coagulation processes of a drop with a film and a jet formation (obtained by the microscope 'Celestron', scale bar = 1 mm).

4. Visualization of capture of some portion of liquid from a sessile drop on a substrate by means by nanosecond spark discharges

Some laboratory experiments require getting a sample of liquid from a sessile drop on a substrate and directing this sample into a capillary with a reagent. Is it possible to do it without touch? Yes, it is possible. One of the methods is generation of nanosecond spark microdischarges between a top of a sessile drop and a reagent meniscus in the capillary.

Some snapshots of the video recording are shown in Fig. 4. A periodic sequence of microsparks was generated between liquids in a drop and a capillary. Microsparks were following each other with a frequency of 40 Hz. The generator based on a cheap HV-module was used for this purpose [34,35]. It generated nanosecond pulses with the amplitude of 5 kV and the length of 100 ns. At the same time, the current in the spark was 400 A.

There was water in a glass capillary with the external diameter of 2.2 mm and the wall thickness of 0.2 mm. The liquid in a sessile drop on a steel substrate is water colored by $KMnO_4$.

It is evident in Fig. 4 that a part of a colored liquid of a drop is captured in a capillary and mixed there for less than 2 s. Mutual attraction of a drop top and a meniscus in a capillary happens before the liquid capture from a drop into a capillary (Fig. 4b), then a liquid bridge is formed (Fig. 4c), the liquid flows from a drop into a capillary by this bridge.

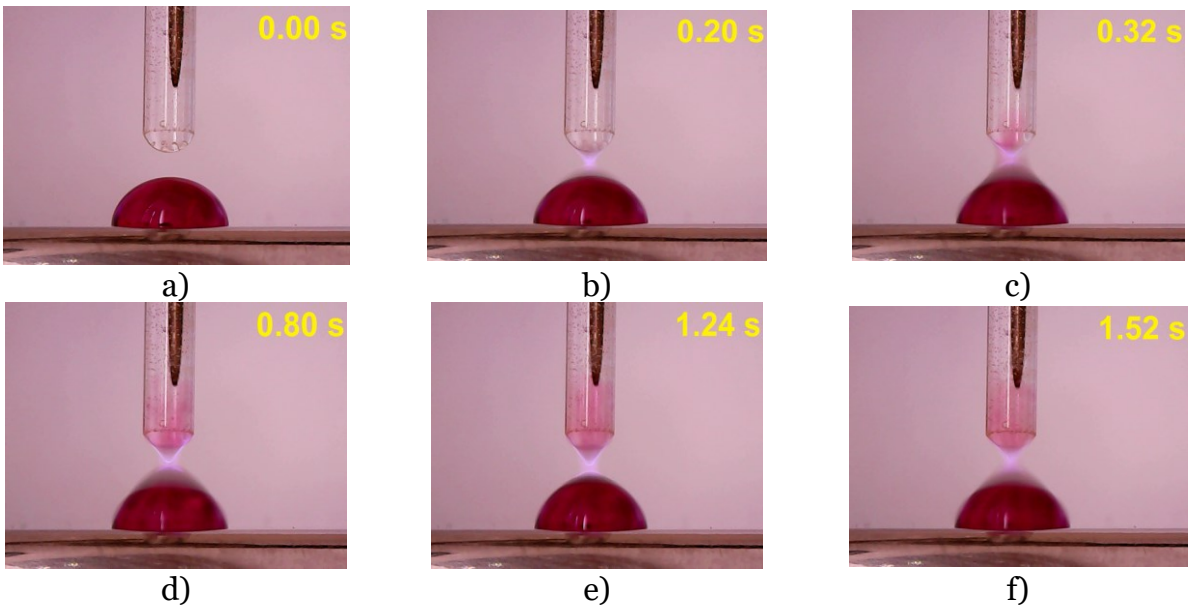

Fig. 4. Snapshots of video-recording of one of the processes of a liquid capture from a drop into a capillary by means of nanosecond spark microdischarges (obtained by the microscope 'Celestron').

There is a question how much liquid crosses a liquid bridge. Several drops were weighed on a digital balance before every experiment and after the bridge formation. It turned out that the drop weight of 20...30 mg was increased in different experiments by 4...17 mg. It means that a transparent jet runs from a capillary to a drop down the bridge, and this jet is stronger than a colored jet going up. However, the transparent jet is not evident in Fig. 4.

Control experiments were carried out to visualize a jet going down. Initially, the water in a drop was transparent, and it was colored in the capillary. There are snapshots of the visualization of a drop going down in Fig. 5, they prove interchange and mixture of drop and capillary liquids.

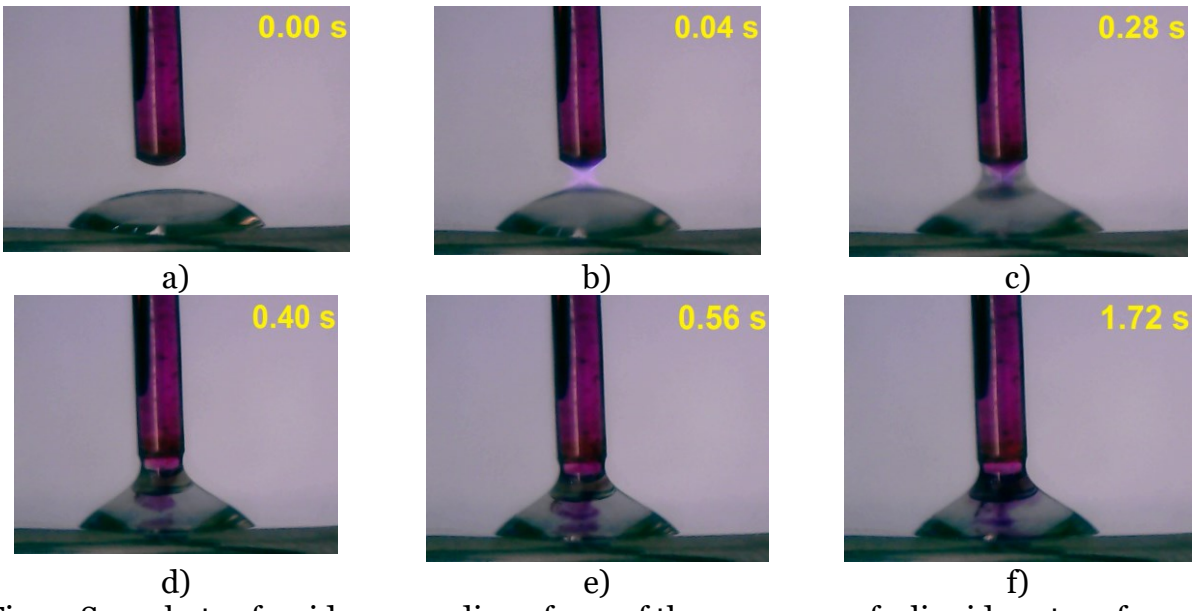

Fig. 5. Snapshots of a video-recording of one of the processes of a liquid capture from a capillary into a drop by nanosecond spark microdischarges (obtained by the microscope 'Celestron').

5. Visualization of nanosecond spark microdischarges in multi -layer transparent structures

Nanosecond microdischarges can be visible like momentary point sparks for an unaided eye. The microscope 'Levenhuk' in a video mode with a frequency of ≤ 7 fps can be used for the detailed visualization of channels of single microdischarges. Let us show it on the sample of the visualization of surface nanosecond microsparks in the work [5], in which surface microdischarges were studied in multi-layer microstructures.

We needed several thin transparent dielectric films to create multi-layer discharge structures; one microhole had to be in each film. A polyethylene film of a 10 μm thickness was chosen as a material.

An auxiliary discharge cell was produced in each film to create a hole. The cell was produced in the following way. Firstly, an electrode was placed on the surface of a standard slide with the sides of $1'' \times 3''$ and thickness of 1 mm. The electrode was cut from aluminum foil of 14 μm thickness by ordinary scissors in the form of a wedge with an angle of ~50^0. This electrode served as an anode. Then, a polyethylene film with dimensions less than the slide dimensions was attached. Then another wedge electrode from aluminum foil was attached to the film to make the distance between the electrode tops 200–400 μm. And at last, all these were covered by one more slide. The obtained sandwich was tightly pressed and strapped by a Scotch tape.

One pulse from a high-voltage generator of a piezoelectric type have been delivered to the electrodes located along different film surfaces (2.5 kV, 40 A, 50 ns). At the same time, a discharge cell was in the air at the atmospheric pressure and room temperature. An electrical breakdown occurred in a film after one pulse. As a result, a circular microhole of ~30 μm diameter was formed after a breakdown. The microhole location is random (between a cathode and an anode). Next pulses just increased the microhole diameter and did not lead to other holes appearance. The process of a circular microhole appearance in a film as a result of an electrical breakdown is shown in Fig. 6.

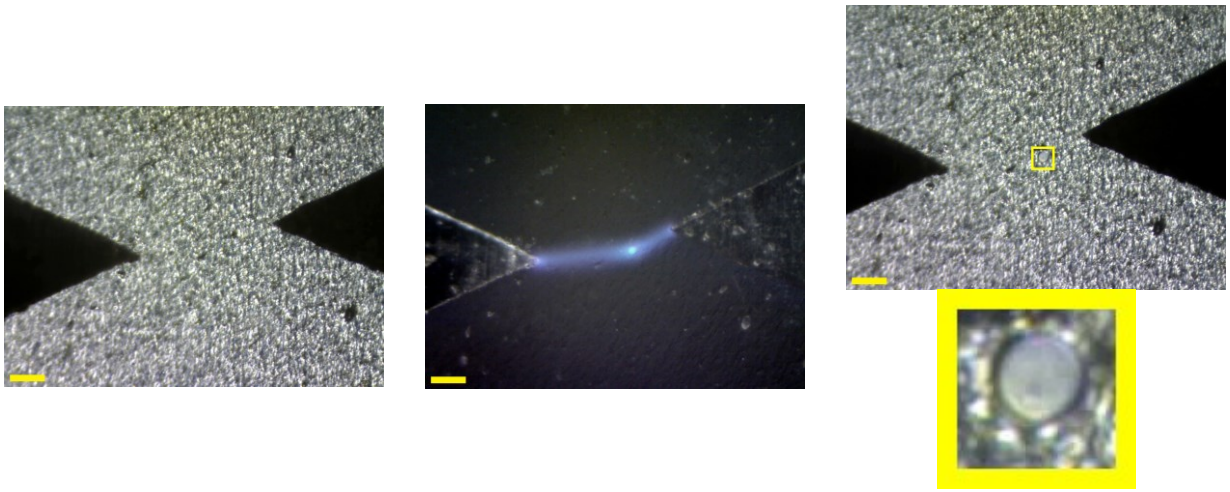

a) b) c)

Fig. 6. The process of a circular microhole appearance in a polyethylene film: a) – an initial film state before a discharge (below light of a film is switched on, a grain pattern of the polyethylene is visible); b) – a film breakdown by an electrical discharge (shooting in darkness); c) – a final state of a film after a discharge with a microhole (below light of a film is switched on, the enlarged cut fragment is below); the cathode is on the left in all photos, scale bar is 100 μm (obtained by the microscope 'Levenhuk'; from [5]).

Let us describe the main results of this work concerning the formation of discharges in multi-layer structures in the form of ***N***-step broken lines. Multi-layer structures were made for this purpose in the same way as in the previous case with the creation of holes.

The order of actions is shown in Fig. 7. Firstly, an electrode from an aluminum foil was placed on the slide surface. Then polyethylene films ($N-1$) with created microholes were attached in the way to make microholes define a specified N-step path of a discharge channel. After this, another wedge electrode from an aluminum foil was attached to the upper film. And at last, all these were covered by one more slide. The obtained sandwich was tightly pressed and strapped by a Scotch tape.

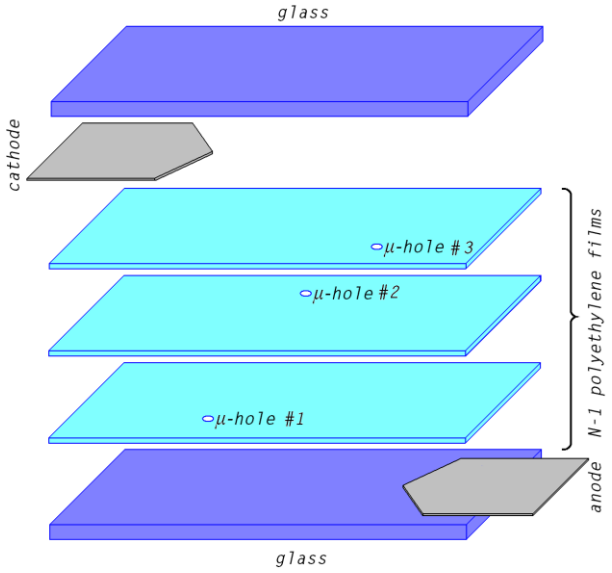

Fig. 7. The order of creation of a multi-layer discharge structure (from [5]).

There are six schemes of different paths (from the left) and six channel images of single nanosecond surface microdischarges corresponding to them (from the right) in Fig. 8. These images are obtained in a darkness, in the air at the atmospheric pressure and room temperature.

A discharge with a V-form channel is shown in Fig. 8a. It has been obtained according to a very simple scheme – with one film.

A discharge with a Z-form channel is shown in Fig. 8b. It has been obtained by means of two films. The channel is formed in the way that electrons move in it not along the electrical field from a cathode to an anode, but they move along another path – firstly, to the microhole # 1 in the first film, then having passed the microhole they move to the microhole # 2 in the second film, and then to the anode. It is discovered in [36] that a discharge can be formed in such a way, that a streamer can move in some definite section perpendicularly to an electrical field. Here we can see that the formation of a Z-form channel on the mean link can be directed almost against the anode direction.

A discharge with an X-form channel obtained by means of two films is shown in Fig. 8c. The discharge channel here has a mean section directed against the field. Besides, the discharge channel has one self-intersection point.

A discharge with a W-form channel obtained by means of three films is shown in Fig. 8d.

A discharge with a star-form channel obtained by means of three films is shown in Fig. 8e. This channel has three self-intersection points.

A discharge with a complex channel obtained by means of four films is shown in Fig. 8f. This channel has two self-intersection points and two links, on which electrons have to move against the field.

It is possible to make the geometry of plasma channels more complex by increasing the number of films.

We should pay attention to a new effect that appears here with assumption that a channel form of a discharge is defined by a streamer trajectory in our multi-layer discharge structure. The effect is the following. Every time when a streamer must pass through a film and then a microhole, it must be oriented and move to the next microhole along the shortest path. This path as we have seen does not often coincide with the electrical field direction, and sometimes can be even directed against the field. But nevertheless, the streamer choses a correct direction to the next microhole. This azimuthal self-orientation of discharge streamers (and as a result, plasma channels) is the main result discovered in this work [5].

6. Current channels of nanosecond spark microdischarges on the surface of living tissues of plants: visualization on a cell-size level

A simple device was constructed to generate surface nanosecond microdischarges. It was produced in the following way [14]. Two electrodes were placed on the surface of a standard slide with the side dimensions of $1'' \times 3''$ and thickness of 1 mm; they were made of an aluminum foil of 14 μm thickness and had a wedge form with an angle of 30^0. The distance between the cathode and anode angle tops could be fixed from 0 to 1 mm. Electrodes were stuck to the slide. Then a studied sample of a living tissue was placed on the electrodes so it has a front side (treated by plasma) turned to the electrodes. Then another slide was attached to the back side of the sample. The device produced in this way in the sandwich form was strapped by a Scotch tape, was turned obversely and could be placed on the microscope stage. There was a slit of 14 μm between a front side of the sample and a slide in the device, in which a surface spark discharge could propagate. Let us note that we didn't use the approach in [37,38] that takes advantage of a variant of a creeping discharge since it was impossible to have a lower light of a transparent sample with a third subjacent discharge.

The microscope 'Levenhuk' was used for detailed visualization of a microdischarge channel. Samples of onion peels (*Allium cepa*) were chosen for microdischarge study along living tissues since onion cells are rather large and are easily observed in the optical microscope. We stuck the electrodes to the slide just before the experiment in a way to have their points at ~ 300 μm from each other in a longitudinal direction and ~ 400 μm in a transverse direction.

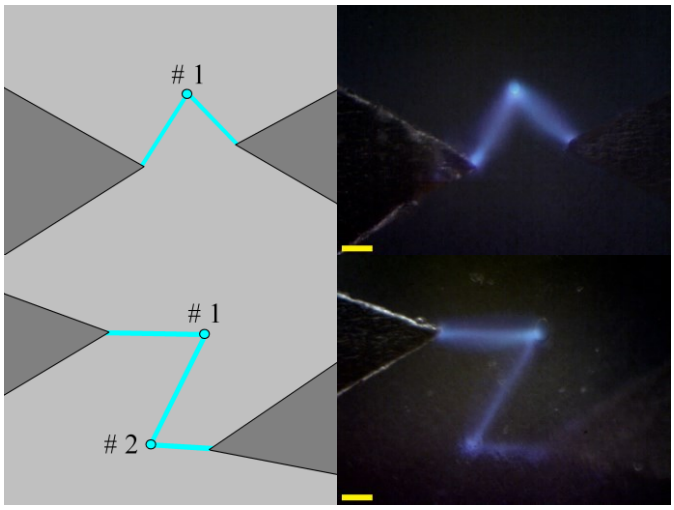

a)

b)

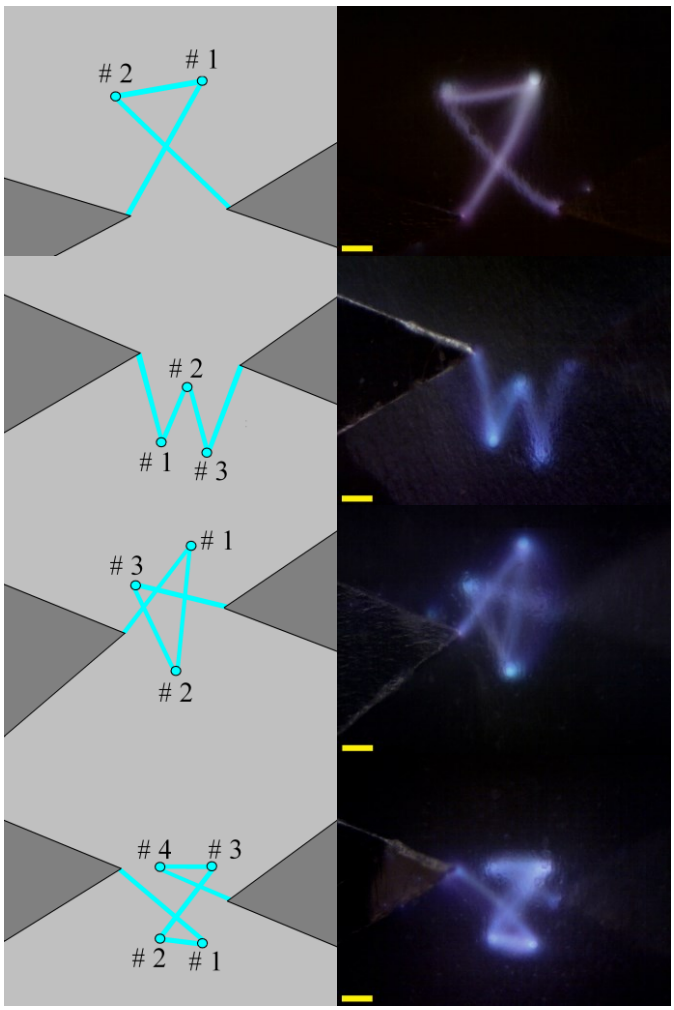

c)

d)

e)

f)

Fig. 8. Scheme of different paths (from the left) and corresponding to them channel images of single nanosecond surface discharges (from the right); the cathode is from the left on all the photos, scale bar – 100 μm): a) – a V-form channel; b) – a Z-form channel; c) – a X-form channel; d) – a W-form channel; e) –a star-form channel; f) – a channel of a complex form (obtained by means of the microscope 'Levenhuk' from [5]).

We prepared samples of onion peels in the following way: firstly, the onion was cut in several parts. Then a thin transparent film was taken from the inner side of an onion petal and was attached to the electrodes. It is known that the increased onion peel due to a squared form of cells reminds a brick wall. The length of an onion cell can be from 250 μm up to 400 μm. We tried to attach the studied sample to the electrodes to make the long cell sides approximately perpendicularly to an interelectrode gap. Let us note that the onion samples were not treated by a coloring agent preliminary, as it is usually practiced in biology.

A single pulse from a high voltage generator of a piezoelectric type (2.5 kV, 40 A, 50 ns) was delivered to the electrodes. Images of plasma discharge channels on the surface of two different samples of onion peels are shown in Figs. 9a,b. It is evident in both cases that a discharge has a zigzag form and propagates along an intercellular envelope. Considering a lattice of the intercellular envelope as a labyrinth, a plasma channel always finds the shortest way in this labyrinth. It agrees with the results in [5] that studies a labyrinth problem solution by plasma of a spark microdischarge in multi-layer structures (see the previous section).

One more interesting phenomenon was discovered during analysis of discharge images. The shortest path in some samples has sections of the reverse current, on which

electrons must move against the electric field. For example, electrons drift to the cathode side on the section AB in Fig. 9b overcoming a potential barrier. Surprisingly, plasma finds an optimal way even at such a labyrinth complication!

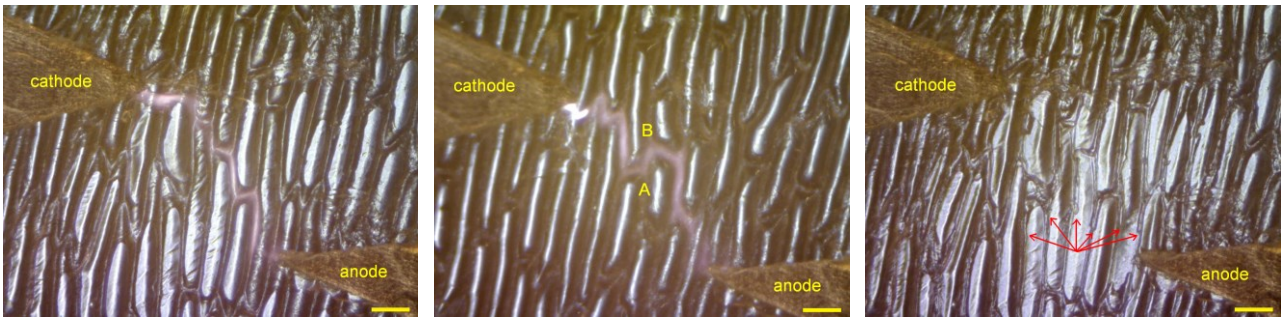

a) b) c)

Fig. 9. Discharge images with a zigzag plasma channel along the surface of an onion peel, scale bar – 100 μm (obtained by means of the microscope 'Levenhuk'):
a) – a simple step discharge; b) – a discharge with a step barrier between the points AB where electrons drift to the cathode side; c) – multiple juice exudations from an intercellular envelope after a single microdischarge on the sample shown in Fig. 9b (arrows show juice jets).

There is such an effect of the cellular tissue on the character of the discharge propagation. But plasma also affects cells. It turned out that a submillijoule energy is enough in a single discharge to break a continuity of the intercellular envelope along the length of a plasma channel and cells attached to the channel. Multiple juice exudations from an intercellular envelope after a single microdischarge are shown in Fig. 9c. After the envelope has been broken, juice starts running from cells. Repeated discharges passing the same optimal path accelerate cell depletion near the current channel. This process can be the basis of the juice and wine production technology [39].

We can suppose that the discovered peculiarities of microdischarges can be the same with other living tissues of other plants. Actually, it turned out that discharge propagation along intercellular envelope of plant tissues is rather typical. Images of microdischarges on plant tissues are provided in Fig. 10: a weed leaf known as Canada water weed, a petal of a day nettle, and a fragment of begonia, correspondingly.

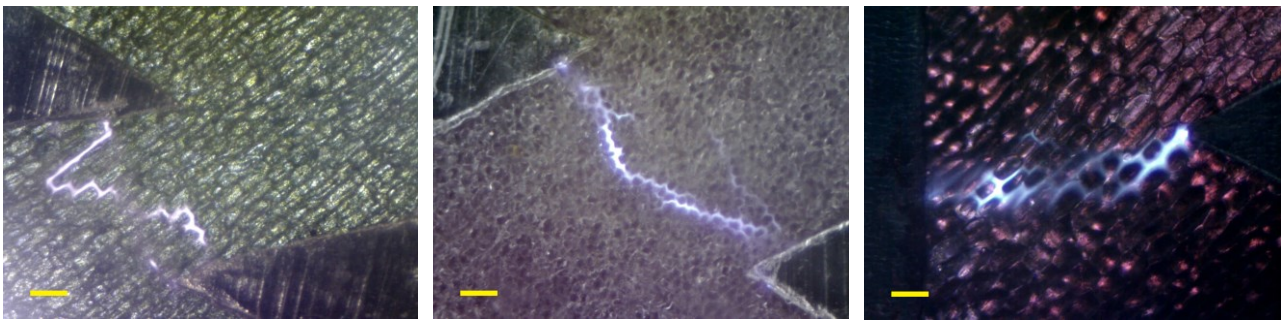

a) b) c)

Fig. 10. Discharge images with zigzag plasma channels along the surface of living tissues of plants: a) – a weed leaf (from [14]); b) – a petal of a day nettle (from [14]); c) – begonia (scale bars – 100 μm; obtained by means of the microscope 'Levenhuk')

7. Visualization of nanosecond spark discharges between grapes

It is known that if two halves of a grape are placed side by side in a microwave oven and the oven is turned on, spark microwave microdischarges occur between the haves [39]. Laboratory tests of such discharges between haves of berries, as well as between hydrogel simulators of berries, have been recently carried out in [40–43]. Electrotechnical characteristics of microwave microdischarges were defined. These studies are within the framework of a new direction in electronic materials science - technologies of advanced materials of edible electronics for medical and pharmaceutical applications [42,44,45].

There is a question, if it is possible to generate unipolar spark discharges between a pair of grapes using them as high-current electrodes? In other words, is a fruit discharger possible?

The hydrogel application as electrode material for low-current edible electronics was studied in [46]. Recently, high-current transparent hydrogel electrodes have been proposed and studied. They can operate in a repetitively pulsed mode of generating nanosecond spark discharges for several minutes with peak currents up to 400 A at a voltage of about 5 kV and a pulse repetition rate of 250 Hz [47,48]. These results motivated us to move from studies of discharges on hydrogel berry simulators to studies of unipolar high-current spark discharges between grapes.

Subsequently, fresh berries of the Taifi blanch grape (Uzbekistan) of an oval shape with the length of 15..20 cm and 10..12 cm in diameter were used as an electrode material. For some experiments, grapes were completely peeled with a microknife, and for some other experiments, only a small area in the form of a square ~1·1 mm was peeled. The berries were strung on the needle electrodes and placed opposite each other at a distance of 1..3 mm from each other.

Electric discharges were formed in the gap after the HV-generator had been turned on in a repetitively pulsed mode with a pulse repetition rate of 50..250 Hz, and a characteristic crack was heard as a result of the generation of shock waves in the air by the discharges. Observations have shown that completely peeled berries (Fig. 11a) and berries (Fig. 11b), peeled on a small area, are providing a consistent stable ignition of spark discharges during a short-time series of pulses with a duration of 1..3 s without any noticeable damage. Thus, the grapes confirmed their performance as high-current electrodes. In this mode, grape electrodes are similar to hydrogel electrodes from [47,48].

a) b)

Fig. 11. Photo images of spark discharges between grapes: a) – completely peeled berries; b) – berries with peeled square areas that are opposite each other (obtained by means of the microscope ‘Celestron’).

To understand the behavior of grapes in long-term (more than 1 min) series, we should recall that berries, like all living plants, have a cellular structure. This structure is a densely packed array of cells, that is, capsules less than 1 mm in size with cytoplasm

(plant juice) and with a nucleus. Cells are separated by thin partitions – intercellular membranes.

It has been previously found that the current of spark discharges along living tissue of plants tends to flow along intercellular partitions [14]. If the discharge current is large enough, then the intercellular partitions are destroyed. This results in the release of juice.

In the experiments described here, the current of spark discharges is approximately 10 times greater than the current in discharges in [14]. Therefore, the discharges intensively destroyed the cells in the pulp of grapes.

If the peel of berries was cut in the form of small squares, drops of juice gradually grew near them. Then the discharges were moving between these drops. The surfaces of the drops approached each other, a liquid bridge was formed between them, then the drops were coagulated, and spark discharges stopped. The process of growth and coagulation of juice drops with the formation of a liquid bridge is shown as a sequence of several frames in Fig. 12. Qualitatively, it is similar to the processes of coagulation of water drops, glycerol, and other liquids observed in [24,25]. The release of liquid from hydrogel electrodes under similar conditions has not been observed in [47,48] since the solid base of the hydrogel (polyacrylamide) turned out to be stronger than the intercellular partitions in grapes. Thus, grape electrodes with a series of pulses of more than 10 s are destroyed inside with the release of juice.

There is a question, why does the surface area of the droplets increase immediately before coagulation? It can be explained. It turns out that when plasma contacts liquid, charged particles, positive ions and electrons settle on its surface. Since the mobility of electrons in plasma is much greater than the mobility of ions, electrons settle much more than ions. As a result, an excess of a negative charge accumulates on the surface of the liquid.

The electron polarizes the liquid around itself forming the so-called hydrated electron state [49,50]. Hydrated electrons repel each other due to the Coulomb interaction, thereby reducing the surface tension of the liquid. In fact, plasma is a specific surfactant [7], which sets the liquid surface in motion increasing the surface area, pushes droplets sitting on the substrate [7,8,11,12], etc. A plasma capillary effect can occur under the influence of plasma [7,9,12].

8. Conclusion

Application of digital optical microscopes for the visualization of single and pulsed-periodic processes in microfluidics and in physics of spark microdischarges is studied. Multiple examples of different processes are provided. Coagulation of a drop sitting on a horizontal substrate with a water film, capture of a drop part by means of nanosecond spark discharges, formation of plasma channels in microdischarges in multilayer transparent structures and along surfaces of living tissues of plants (on a cell-level), microdischarges formation between grapes are among them.

Accumulated long-term experience allowed us to highlight some important moments in the digital optical microscopy to visualize the physical processes in the microfluidics and in spark microdischarge technique:

– digital microscopes require preliminary calibration by means of the special measurement dot matrices (test patterns), which allow determining the number of pixels per length unit. At that, vertical and horizontal calibration ratios of the image could be different;

– it is necessary to provide special illumination of the studied objects and minimize the disturbing factors like shadows or blinks. For this purpose, one can use colored LED. It is necessary to take into account that the higher the frame rate, the brighter illumination should be provided for the recording;

– it is necessary to minimize the electromagnetic noise, which initiates operation malfunction of the digital microscopes; for this purpose, one can use electromagnetic filters, ground connection, and shields;
– it is possible to use quick-dissolving dyes for contrast enhancement of small liquid volumes; one should remember that dyes can change properties of the studied liquids;
– for the study lasting more than 1 min, it is necessary to take into account that the liquid drops could significantly change their volume at the expense of evaporation; in some cases, it is possible to use heavy liquids (glycerin, for example) instead of water.

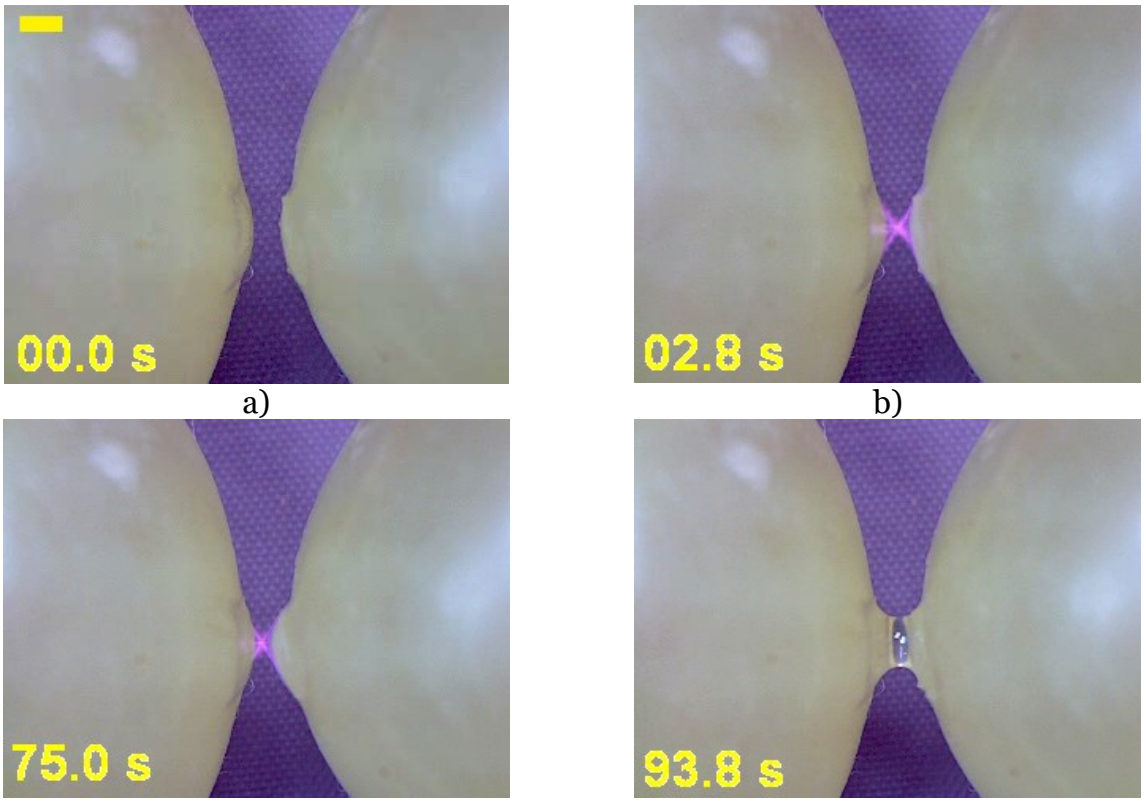

a) b) c) d)

Fig. 12. Separate frames of the video recording of the process of extracting juice drops and their coagulation with the formation of a liquid bridge (the time is counted from the moment the HV generator is turned on: a) – initial state; b)–c) – counter growth of drops; d) – coagulation with the formation of a liquid bridge (obtained by means of the microscope 'Celestron', scale bar – 1 mm).

References

[1] Friend J. and Yeo L.Y. Microscale acoustofluidics: Microfluidics driven via acoustics and ultrasonics / Rev. Mod. Phys. 2011. V. 83. № 2. P. 647–703.
[2] Convery N. and Gadegaard N. 30 years of microfluidics / Micro Nano Eng. 2019. V. 2. № 1. P. 76–91.
[3] Iza F., Kim G.J., Lee S.M., Lee J.K., Walsh J.L., Zhang Y.T., and Kong M.G. Microplasmas: Sources, particle kinetics, and biomedical applications / Plasma Proc. Polymers. 2008. V. 5. № 4. P. 322–344.
[4] Schoenbach K.H. and Becker K. 20 years of microplasma research: a status report / Euro. Phys. J. D. 2016. V. 70. № 2. P. 29-1–22.
[5] Dubinov A.E. and Lyubimtseva V.A. Nanosecond surface microdischarges in multilayer structures / J. Eng. Phys. Thermophys. 2018. V. 91. № 2. P. 531–536.

[6] Dubinov A.E., Kozhayeva J.P., L'vov I.L., Sadovoy S.A., Selemir V.D., and Vyalykh D.V. Rapid crystallization of natural sugars in bee's honey under the influence of nanosecond microdischarges / Cryst. Growth Des. 2015. V. 15. № 10. P. 4975–4978.
[7] Dubinov A.E., Kozhayeva J.P., Lyubimtseva V.A., and Selemir V.D. Plasma as a surfactant: A new capillary effect and a new wetting effect induced by nanosecond spark discharges / IEEE Trans. Plasma Sci. 2017. V. 45. № 12. P. 3094–3099.
[8] Dubinov A.E., Kozhayeva J.P., Lyubimtseva V.A., and Selemir V.D. Peristaltic motion of liquid droplets along metal surfaces under the influense of plasma of nanosecond spark micro discharges / Magnetohydrodynamics. 2018. V. 54. № 3. P. 261–275.
[9] Dubinov A.E., Kozhayeva J.P., and Selemir V.D. Plasma capillary effect / High Temp. 2018. V. 56. № 3. P. 451–453.
[10] Dubinov A.E. and Lyubimtseva V.A. Crystallization features of aqueous solutions in their droplets evaporated by nanosecond spark discharge treatment / High Energy Chem. 2019. T. 53. № 1. C. 1–4.
[11] Dubinov A.E., Iskhakova D.N. and Lyubimtseva V.A. An inversion of contact angle hysteresis when a liquid drop slides up on an inclined plane under the spark discharge action / Phys. Fluids. 2021. V. 33. № 6. P. 061707-1–4.
[12] Dubinov A.E., Kozhayeva J.P., Lyubimtseva V.A., and Selemir V.D. Hydrodynamic and physicochemical phenomena in liquid droplets under the action of nanosecond spark discharges: A review / Adv. Colloid Interface Sci. 2019. V. 271. № 1. P. 101986-1–32.
[13] Dobrynin D., Arjunan K., Fridman A., Friedman G., and Clyne A.M. Direct and controllable nitric oxide delivery into biological media and living cells by a pin-to-hole spark discharge (PHD) plasma / J. Phys. D: Appl. Phys. 2011. V. 44. № 7. P. 075201-1–10.
[14] Kozhayeva J.P., Lyubimtseva V.A., Zuimatch E.A., and Dubinov A.E. A novel insight on the geometry of plasma channels of nanosecond micron-size discharges on the surface of living tissues of plants / Plasma Proc. Polymers. 2015. V. 12. № 3. P. 293–296.
[15] Kumagai S., Chang C.-Y., Jeong J., Kobayashi M., Shimizu T., and Sasaki M. Development of plasma-on-chip: Plasma treatment for individual cells cultured in media / Jap. J. Appl. Phys. 2016. V. 55. № 1S. P. 01AF01-1–8.
[16] Dubinov A.E., Kozhayeva J.P., and Lyubimtseva V.A. Simple device to study influence of nanosecond surface microdischarge plasma on biomaterials / IEEE Trans. Plasma Sci. 2015. V. 43. № 9. P. 3224–3227.
[17] Znamenskaya I.A., Sysoev N.N., and Doroshchenko I.A. Animations analysis in experimental fluid dynamics / Sci. Visualization. 2021. V. 13. № 4. P. 66–75.
[18] Mursenkova I.V., Liao Yu., Ulanov P.Yu, and Shi L. High-speed shadowgraphy of the interaction of an oblique shock wave in a channel with a surface sliding discharge / Sci. Visualization. 2021. V. 13. № 3. P. 47–57.
[19] Dubinov A.E., Pylayev N.A., Sadovoy S.A., and Sadchikov E.A. HD-Image of nanosecond microspark / IEEE Trans. Plasma Sci. 2014. V. 42. № 10. P. 2648–2649.
[20] Sudeepthi A., Nath A., Yeo L.Y., and Sen A.K. Coalescence of droplets in a microwell driven by surface acoustic waves / Langmuir. 2021. V. 37. № 4. P. 1578–1587.
[21] Nilsson M.A. and Rothstein J.P. The effect of contact angle hysteresis on droplet coalescence and mixing / J. Colloid Interface Sci. 2011. V. 363. № 2. P. 646–654.
[22] Borcia R. and Bestehorn M. On the coalescence of sessile drops with miscible liquids / Eur. Phys. J. E. 2011. V. 34. № 8. P. 81-1–9.
[23] Sykes T.C., Castrejón-Pita A.A., Castrejón-Pita J.R., Harbottle D., Khatir Z., Thompson H.M., and Wilson M.C.T. Surface jets and internal mixing during the coalescence of impacting and sessile droplets / Phys. Rev. Fluids. 2020. V. 5. № 2. P. 023602-1–21.

[24] Rowland S.M. and Lin F.C. Stability of alternating current discharges between water drops on insulation surfaces / J. Phys. D: Appl. Phys. 2006. V. 39. № 14. P. 3067–3076.
[25] Dubinov A.E., Kozhayeva J.P., Golovanov V.V., and Selemir V.D. Coalescence of liquid droplets under effect of pulsed-periodic spark discharges / IEEE Trans. Plasma Sci. 2019. V. 47. № 1. P. 76–80.
[26] Karpitschka S. and Riegler H. Quantitative experimental study on the transition between fast and delayed coalescence of sessile droplets with different but completely miscible liquids / Langmuir. 2010. V. 26. № 14. P. 11823–11829.
[27] Karpitschka S., Hanske C., Fery A., and Riegler H. Coalescence and noncoalescence of sessile drops: Impact of surface forces / Langmuir. 2014. V. 30. № 23. P. 6826–6830.
[28] Ludwicki J.M. and Steen P.H. Sweeping by sessile drop coalescence / Eur. Phys. J. ST. 2020. V. 229. № 10. P. 1739–1756.
[29] Pearson R.S. Manganese color reactions / J. Chem. Educ. 1988. V. 65. № 5. P. 451–452.
[30] Lincoln J. Electric field patterns made visible with potassium permanganate / Phys. Teacher. 2017. V. 55. № 2. P. 74–75.
[31] Ching J.-H., Chen P., and Tsai P.A. Convective mixing in homogeneous porous media flow / Phys. Rev. Fluids. 2017. V. 2. № 1. P. 014102-1–9.
[32] Proust S. and Nikora V.I. Compound open-channel flows: effects of transverse currents on the flow structure / J. Fluid Mech. 2020. V. 885. № 1. P. A24-1–38.
[33] Sivasubramanian M., Jaganathan K.D., and Ramkumar P. Experimental investigation of flow visualization of vortex shedding on a flow over square block / Materials Today: Proceedings. 2021. V. 46. № 17. P. 7676–7681.
[34] Nath R., Patidar M.M., Ghodke N.K., Das S.C., and Ganesan V. An innovation in corona charging of electrets / Asian J. Converg. Technol. 2020. V. 6. № 2. P. 28–32.
[35] Dubinov A.E. and Lyubimtseva V.A. Triggering of Venus Flytrap with nanosecond spark discharges / IEEE Trans. Plasma Sci. 2022. V. 50. № 6. P. 1710–1714.
[36] Reyes D.R., Ghanem M.M., Whitesides G.M., and Manz A. Glow discharge in microfluidic chips for visible analog computing / Lab on a Chip. 2002. V. 2. № 2. P. 113–116.
[37] Louste C., Artana G., Moreau E., and Touchard G. Sliding discharge in air at atmospheric pressure: electrical properties / J. Electrostatics. 2005. V. 63. № 6–10. P. 615–620.
[38] Dubinov A.E. A particle-in-cell simulation of a process of avalanche developing at a non-completed sliding discharge / Plasma Sources Sci. Techn. V. 9. № 4. P. 597–599 (2000).
[39] Sack M., Sigler J., Eing C., Stukenbrock L., Stängle R., Wolf A., and Müller G. Operation of an electroporation device for grape mash / IEEE Trans. Plasma Sci. 2010. V. 38. № 8. P. 76–80.
[40] Khattak H.K., Bianucci P., and Slepkov A.D. Linking plasma formation in grapes to microwave resonances of aqueous dimmers / Proc. Nat. Acad. Sci. 2019. V. 116. № 10. P. 4000–4005.
[41] Khattak H.K., Waitukaitis S.R., and Slepkov A.D. Microwave induced mechanical activation of hydrogel dimmers / Soft Matter. 2019. V. 15. №29. P. 5804–5809.
[42] Slepkov A. D. Fruit photonics and the shape of water / Phys. Today. 2020. V. 73. № 6. P. 62–63.
[43] Lin M.S., Liu L.C., Barnett L.R., Tsai Y.F., and Chu K.R. On electromagnetic wave ignited sparks in aqueous dimmers / Phys. Plasmas. 2021. V. 28. № 10. P. 102102-1–11.

[44] Wu Y., Ye D., Shan Y., He Y., Su Z., Liang J., Zheng J., Yang Z., Yang H., Xu W., and Jiang H. Edible and nutritive electronics: Materials, fabrications, components, and applications / Adv. Mater. Technol. 2020. V. 5. № 10. P. 2000100-1–28.
[45] Sharova A.S., Melloni F., Lanzani G., Bettinger C.J., and Caironi M. Edible electronics: The vision and the challenge / Adv. Mater. Technol. 2021. V. 6. № 2. P. 2000757-1–39.
[46] Keller A., Pham J., Warren H., and in het Panhuis M. Conducting hydrogels for edible electrodes / J. Mater. Chem. B. 2017. V. 5. № 27. P. 5318–5328.
[47] Dubinov A.E. and Kozhayeva J.P. Generating periodic pulse sequences of nanosecond spark discharges in an air gap between transparent hydrogel electrodes / Techn. Phys. Lett. 2019. V. 45. № 4. P. 383–385.
[48] Dubinov A.E. and Kozhayeva J.P. Transparent hydrogel electrodes as a new class of electrodes for high-current nanosecond atmospheric-pressure discharges / High Energy Chem. 2019. V. 53. № 6. P. 425–428.
[49] Gopalakrishnan R., Kawamura E., Lichtenberg A.J., Lieberman M.A., and Graves D.B. Solvated electrons at the atmospheric pressure plasma–water anodic interface / J. Phys. D: Appl. Phys. 2016. V. 49. № 29. P. 295205-1–13.
[50] Martin D.C., Bartels D.M., Rumbach P., and Go D.B. Experimental confirmation of solvated electron concentration and penetration scaling at a plasma–liquid interface / Plasma Sources Sci. Techn. 2021. V. 30. № 3. P. 03LT01-1–6.